

Frequency of spring dust weather in North China linked to sea ice variability in the Barents Sea

Ke Fan^{1,2,5}  · Zhiming Xie¹ · Huijun Wang² · Zhiqing Xu^{1,3} · Jiping Liu⁴

Received: 8 July 2016 / Accepted: 23 December 2016 / Published online: 8 February 2017
© Springer-Verlag Berlin Heidelberg 2017

Abstract The link between winter sea ice cover in the Barents Sea (SICBS) and the frequency of spring dust weather over North China (DWFNC) is investigated. It is found that year-to-year variability of SICBS and DWFNC are strongly correlated for the period 1996–2014 with a correlation coefficient of -0.65 , whereas the correlation between SICBS and DWFNC is not statistically significant for the periods 1980–2014 and 1980–1995. During 1996–2014, low winter SICBS is associated with decreased snow cover over western Siberia (SCWS) in both winter and spring, which is also supported by a strengthening relationship between winter SICBS and spring SCWS since the mid-1990s. This leads to changes in atmospheric circulation and climate conditions that are favorable for increased frequency of dust weather events over North China. Our further analysis suggests that the interannual variability of the standard deviation of SICBS has intensified and the center of actions has moved eastward to the north Barents

Sea and Kara Sea since the mid-1990s. Such change may easily induce stronger and southward stationary Rossby wave train propagation, influencing the dust-related atmospheric circulation (strengthened East Asian subtropical jet, increased cyclogenesis, and larger atmospheric thermal instability). Thus interannual variation of winter SICBS plays an increasingly important role in dust-related climate conditions over North China, which might serve as a new precursor for the prediction of spring dust activity in North China.

Keywords Winter sea-ice cover · Barents Sea · Dust weather frequency · North China · Snow cover · Western Siberia

1 Introduction

Dust storms, a weather phenomenon that mainly occurs in spring (March, April, and May) in northern China, are related to strong winds, thermal instability, and dust sources. Strong dust events can reach the North Pacific, Japan, Korea, and even North America, affecting human health and the environment. Dust aerosol particles can also influence weather and climate through radiative effects and cloud microphysical processes. The variability of dust events is influenced by climate conditions and erodibility of dust source. Previous studies have shown that the long-term variation in dust weather frequency (DWF) in China has exhibited a negative trend in recent decades, with high frequency from the 1950s to the 1970s, low frequency from the 1980s to the 1990s, and a remarkable increase in frequency during 2000–2002 (Qian et al. 2002; Kurosaki and Mikami 2003; Fan and Wang 2004, 2006, 2007a, b; Zhao et al. 2004; Kang and Wang 2005; Fan et al. 2016). The

✉ Ke Fan
fanke@mail.iap.ac.cn

¹ Nansen-Zhu International Research Centre, Institute of Atmospheric Physics, Chinese Academy of Sciences, Beijing 100029, China

² Collaborative Innovation Center on Forecast and Evaluation of Meteorological Disasters, Nanjing University of Information Science & Technology, Nanjing 210044, China

³ Climate Change Research Center, Chinese Academy of Sciences, Beijing 100029, China

⁴ Department of Atmospheric and Environmental Sciences, University at Albany, State University of New York, Albany, NY, USA

⁵ University of the Chinese Academy of Sciences, Beijing 100049, China

interannual and interdecadal variation of DWF in northern China are associated with the intensity of the East Asian winter monsoon (Kang and Wang 2005; Wu et al. 2010), surface winds over East Asia (Kurosaki and Mikami 2003), the cyclone frequency in northern China (Qian et al. 2002; Zhu et al. 2008), surface vegetation and aeolian dust source (Zhou and Zhao 2004), the status of the El Niño/Southern Oscillation (ENSO) (Zhang, 2002), and the Antarctic Oscillation (AAO) (Fan and Wang 2004, 2007a, b). Lang (2008) developed an effective operational climate prediction model for DWF in northern China, in which the AAO, Arctic Oscillation (AO), East Asian winter monsoon, ENSO, and other dust-related climate indices are used as predictors.

The rapid decline of Arctic sea-ice cover (SIC) has been well documented (e.g., Stroeve et al. 2007; Cosmisio et al. 2008). Its impacts on the mid- and high-latitude weather and climate have been investigated (e.g., Wu et al. 1999; Comiso et al. 2008; Deser and Teng 2008; Liu et al. 2012; Francis and Vavrus 2012; Cohen et al. 2014). The loss of Arctic SIC may have increased the frequency of cold winters over Eurasia (e.g., Honda et al. 2009; Petoukhov and Semenov 2010; Inoue and Hori 2012; Liu et al. 2012; Gao et al. 2015), and intensified haze pollution in eastern China by changing the regional atmospheric circulation (Wang et al. 2015). Considering the substantial loss of Arctic SIC in recent years, and the fact that dust event activity in northern China is strongly influenced by regional atmospheric circulation (Fan and Wang 2004, 2006; Kang and Wang 2005), the question is whether the profound change in winter Arctic SIC has recognizable impacts on spring DWF in northern China.

The paper is organized as follows. Section 2 describes the datasets used in this study. Section 3.1 examines the relationship between winter SIC in the Barents Sea (SICBS) and spring DWF in North China (DWFNC), and their corresponding winter and spring atmospheric circulation and climate conditions. Section 3.2 shows how winter SICBS is connected to the DWFNC in the following spring and the potential role of winter and spring snow cover over western Siberia in the linkage between winter SICBS and spring DWFNC. Section 3.3 discusses why winter SICBS has been significantly correlated with spring DWFNC since the mid-1990s. Finally, a concluding remark is given in Sect. 4.

2 Data

Monthly atmospheric reanalysis data from the National Centers for Environmental Prediction and the National Center for Atmospheric Research (NCEP/NCAR) at a resolution of 2.5° is used (Kalnay et al. 1996). The monthly

SIC data is obtained from the Met Office Hadley Centre for Climate Prediction and Research, with a resolution of 1° . The monthly soil moisture data, with a resolution of 0.5° , is obtained from the Climate Prediction Center of the National Oceanic and Atmospheric Administration. The monthly averaged number of days of dust weather at 53 weather stations in North China during 1961–2014, are obtained from the National Climate Information Center in China. The dust weather can be classified into three categories (dust haze, blowing dust, and dust storm) mainly based on the horizontal visibility as the dust weather occurs. The range of horizontal visibility for dust haze, blowing dust, and dust storm is <10 , $1\text{--}10$, and <1 km, respectively.

The months of December–February (DJF) and March–May (MAM) are used to calculate winter and spring means, respectively. The index of SICBS is calculated as the area-averaged SIC in the region ($74^\circ\text{--}77^\circ\text{N}$, $30^\circ\text{--}60^\circ\text{E}$). The index of DWFNC is defined as the averaged number of days of dust weather that occur at 53 weather stations in North China ($35^\circ\text{--}42^\circ\text{N}$, $105^\circ\text{--}120^\circ\text{E}$, see the domain in Fig. 2c, d). The snow cover data is obtained from the Rutgers University Global snow Lab (Robinson et al. 1993). The index of snow cover over western Siberia (SCWS) is calculated as the area-averaged snow cover in the region of $54^\circ\text{--}60^\circ\text{N}$, $60^\circ\text{--}80^\circ\text{E}$. The precipitation data is obtained from the NOAA's Precipitation Reconstruction over Land (PREC/L) at a resolution of 2.5° . The daily zonal wind data is obtained from ERA-Interim at a resolution of 1.5° for the period January 1979 to December 2015. The common period for all the datasets is from 1980 to 2014. For the composite analysis, the years 2000, 2001 and 2002 (1998, 2003 and 2004) are selected as low (high) SICBS years, and the years 2000, 2001, 2002 and 2006 (1997 and 2003) are selected as high (low) DWFNC years (Fig. 1a).

3 Results

3.1 Winter and spring atmospheric circulation and climate factors

Figure 1a shows the time series of winter SICBS and spring DWFNC from 1980 to 2014. Winter SICBS and spring DWFNC (dashed lines) exhibit strong interannual variability superimposed on a declining trend during 1980–2014. It appears that variations in SICBS and DWFNC are relatively more in-phase before 1995. The opposite is the case (out-of-phase) after 1995. The correlations between SICBS and DWFNC are 0.13 for the entire period, 0.34 during 1980–1995, and -0.35 during 1996–2014, but they are not statistically significant. However, when the linear trend is removed from both time series (solid lines), the correlation

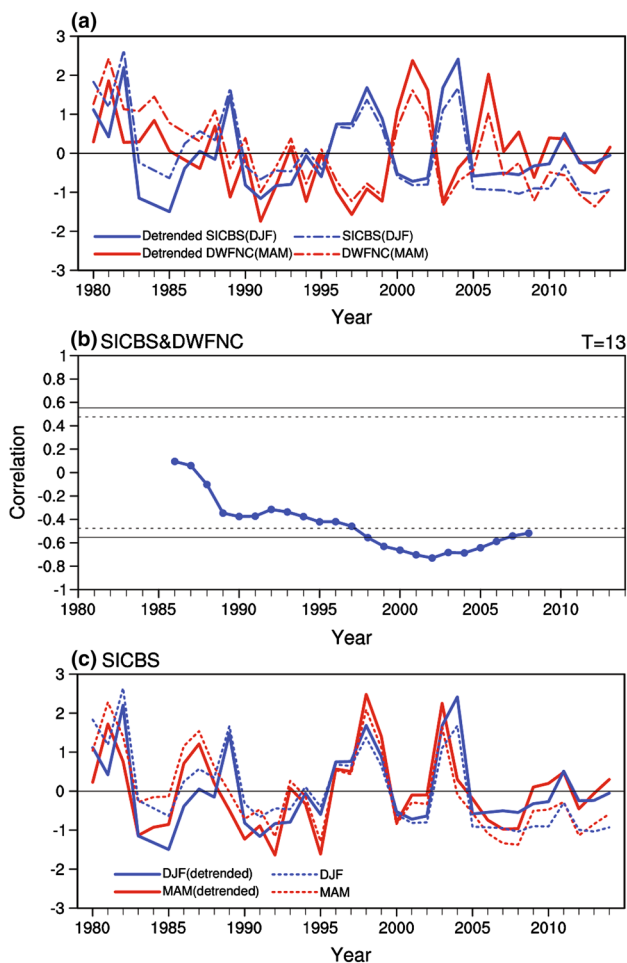


Fig. 1 **a** Time series of normalized winter SICBS (blue) and spring DWFNC (red), without (solid lines) and with (dashed lines) linear trends. **b** The 13-year-sliding correlation coefficient between detrended winter SICBS (blue) and detrended spring DWFNC. **c** Time series of the normalized winter (blue) and spring SICBS (red), with (dashed lines) and without (solid lines) the linear trends. The dashed and solid lines denote correlations required for significance at the 90 and 95% levels, respectively, as estimated using a Student's *t* test

between SICBS and DWFNC is increased substantially to -0.65 for the period 1996–2014, exceeding the 99% significant level (Fig. 1a; Table 1), whereas the correlations for 1980–2014 (-0.32) and 1980–1995 (0.07) remain insignificant (Table 1). Here we calculate 13-year sliding correlation coefficients between the detrended SICBS and DWFNC. As shown in Fig. 1b, the correlation becomes stronger and statistically significant after the mid-1990s.

Figure 2a, b show the linear regressions of the detrended spring DWFNC on the detrended winter SIC at each grid in the northern Norwegian, Barents and Kara Seas during 1980–1995 (hereafter referred to as P1) and 1996–2014 (hereafter referred to as P2), respectively. During P2, SIC anomalies in large parts of the Barents Sea show a strong

out-of-phase relationship with DWFNC, statistically significant exceeding the 95% level. In contrast, during P1, only scattered significant negative correlations are found in the Barents Sea. We also calculate the correlation between winter SICBS and spring DWF at each weather observation station in North China during P1 and P2 (Fig. 2c, d). Although DWF at all weather stations in North China is negatively correlated with SICBS for both P1 and P2, widespread significant negative correlations only appear during P2 (shaded in Fig. 2d). The detrended SICBS anomalies show good persistence from winter to spring, with the correlation coefficient of 0.74 (0.67), 0.66 (0.55), 0.83 (0.76) during 1980–2014, 1980–1995 and 1996–2014, respectively (above the 99% significant level, Fig. 1c). Thus we speculate that winter SICBS has played an important role in the interannual variability of spring DWFNC since the mid-1990s.

To investigate how atmospheric circulation is associated with winter SICBS and spring DWFNC since the mid-1990s, we first regress the sea level pressure (SLP) and wind fields at 850 and 200 hPa in DJF and MAM on SICBS and DWFNC, separately, for the period 1996–2014. Note all data are detrended and SICBS is multiplied by -1 for a clear comparison. In DJF (Fig. 3), associated with decreased SICBS and increased DWFNC, the SLP is substantially lower over Europe and higher over Siberia (60° – 90° N, 60° – 120° E, Fig. 3a, b). This is accompanied by an anomalous cyclonic and anticyclonic circulation over these two regions at 850 and 200 hPa (Fig. 3c–f), respectively, together with a stronger upper-level subtropical East Asian Jet (EASJ), which is climatologically anchored over East Asia and the western Pacific, with a maximum wind speed over the south of Japan (Yang et al. 2002). As a result, the low-level southwesterly winds associated with the anomalous cyclonic circulation advect warm and moist air mass from the north Atlantic and the Norwegian Sea to the Barents Sea and Europe. This reduces sea ice in the Barents Sea and increases surface temperature over Europe (Figs. 3c, d, 5a). Meanwhile, the northerly winds at the front of the anomalous anticyclonic circulation over Siberia brings cold and dry air southward into the east of Baikal, Mongolia, and North China, leading to a cooling in these areas (Figs. 3c, d, 5a).

In MAM (Fig. 4), associated with decreased SICBS and more DWFNC, the aforementioned anomalous cyclonic and anticyclonic circulations move eastward relative to those in DJF (Figs. 3, 4). The SLP anomalies in the North Atlantic look like a negative phase North Atlantic Oscillation (NAO) pattern, characterized by positive SLP anomalies in the North Atlantic sector of the Arctic and negative SLP anomalies in the mid-latitudes of eastern north Atlantic and Europe. It seems that the negative SLP anomalies extend eastward from Lake Baikal, through Mongolia, to

Fig. 2 **a, b** Linear regression of the gridpoint winter SIC on spring DWFNC during **a** 1980–1995 and **b** 1996–2014. **c, d** Correlation between spring DWF at weather observation stations in North China with winter SICBS during **c** 1980–1995 and **d** 1996–2014, in which the weather observation stations are denoted by dots. The linear trends have been removed. The *dotted* (**a, b**) and *shaded* (**c, d**) region represent correlations required for significance at the 95% level, as estimated using a Student's *t* test

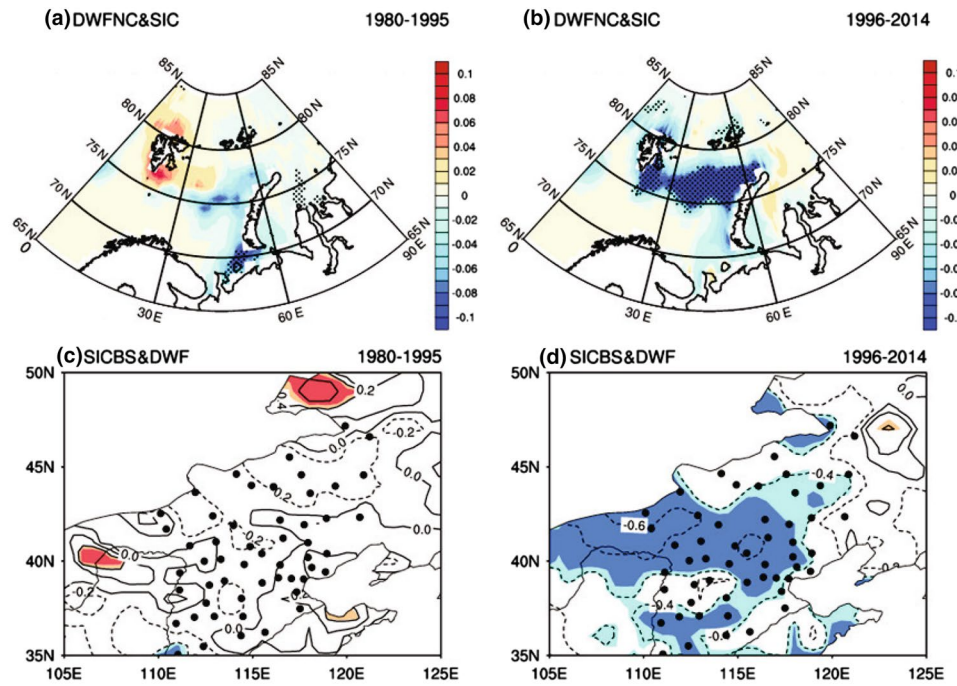


Table 1 Correlation coefficients between winter SICBS and spring DWFNC, and between winter SICBS and spring SCWS, for 1980–2014, 1980–1995, and 1996–2014, respectively, with and without trends. Statistical significance at the 95% (*) and 99% (**) level, as estimated using a Student's *t* test (all other values are below the 90% level)

	1980–2014	1980–1995	1996–2014
DWFNC&SICBS- DJF (without trend)	0.13 (–0.33)	0.34 (0.07)	–0.35 (–0.65**)
SICBS- DJF&SCWS- MAM (without trend)	0.43* (0.35*)	0.12 (0.02)	0.69** (0.6**)

Northeast Asia, which are closely associated with cyclogenesis and frontogenesis (Fig. 4a, b). As a result, a strong cyclonic anomaly at 850 hPa dominates over the east of Mongolia, North China, Korea, and Japan (Fig. 4c, d), accompanied by a stronger EASJ [(25°–35°N, 100°–50°E)] (Fig. 4e, f). Previous studies suggested that the stronger EASJ favors westerly momentum transported downward from upper levels, which results in stronger surface winds and low-level cyclogenesis and frontogenesis, providing favorable dynamic conditions for increased DWFNC (Uccellini 1986; Fan and Wang 2004, 2006, 2007a, b).

Previous studies have shown that cold temperatures in winter are favorable for more spring dust weather (Qian et al. 2002; Zhang et al. 2002; Fan and Wang 2004). In northern China, cold anomalies in winter can lead to a deeper frozen soil layer, resulting in serious desertification

when warm anomalies set in. Deficient spring precipitation and dry soil moisture in northern China also provide more dust sources. Figure 5 shows the composite difference in winter and spring surface air temperature (SAT), precipitation and soil moisture between less and more winter SICBS years (less minus more). In winter, decreased SICBS and increased DWFNC correspond to a warming in Europe and the Arctic and a cooling in eastern Siberia, Mongolia and North China. This is also accompanied by increased precipitation over Europe and decreased precipitation over West Asia and North China (Fig. 5a–d). These changes are generally consistent with previous findings (Honda et al. 2009; Inoue and Hori 2012; Francis and Vavrus 2012; Liu et al. 2012). Because of the aforementioned temperature and precipitation changes, soil moisture tends to be wetter in eastern Europe and west Siberia and dryer in southern Asia and northern China, when sea ice is anomalously low in the Barents Sea (Fig. 5e) and the frequency of dust weather is anomalously high over North China (Fig. 5f). Moreover, anomalies in the aforementioned climate variables in MAM related to decreased SICBS are similar to those identified in DJF, but the strongest warming shift eastwards to central Siberia and Western Siberia becomes dryer, which decreased snow cover in these regions. Vegetation coverage in northern China is an important factor influencing the frequency of spring dust weather events. Low vegetation cover increases the occurrence of dust storm (e.g., Zuo and Zhai 2004). In MAM, vegetation cover also decreases in North China (not shown) due to decreased precipitation and dryer soil moisture conditions. Therefore, the aforementioned changes in climate conditions from winter and spring

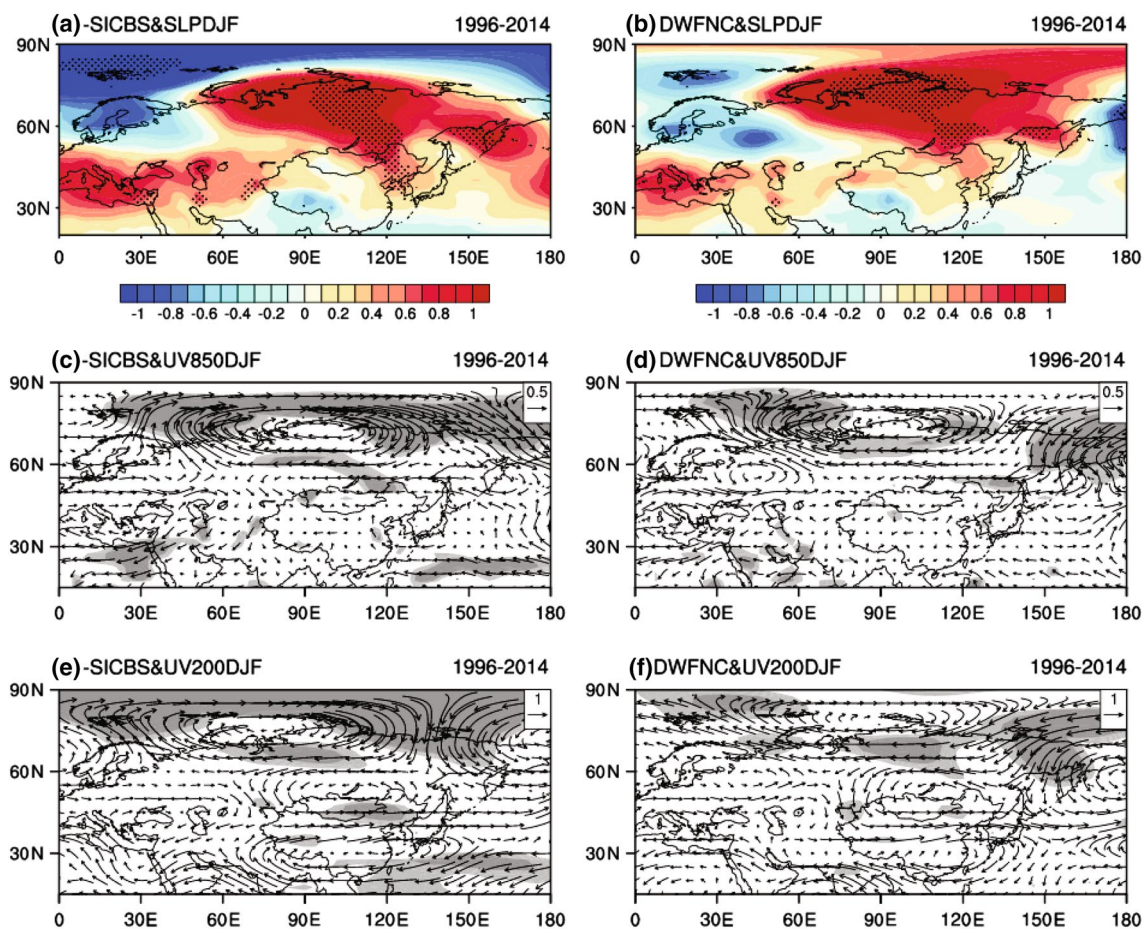


Fig. 3 Linear regression of gridpoint **a, b** DJF-SLP (units: millibars), **c, d** DJF-UV 850 hPa (units: $m s^{-1}$) and **e, f** DJF-UV 200 hPa (units: $m s^{-1}$), on **(a, c, d)** negative winter SICBS and **b, d, f** spring DWFNC, during 1996–2014. The linear trends have been removed

and SICBS multiplied by -1 . The *dotted* (**a, b**) and *shaded region* represent correlations required for significance at the 95% level, as estimated using a Student's *t* test

associated with negative SICBS anomalies are favorable for increased DWFNC. Moreover, the atmospheric circulation and climate conditions in winter and spring under negative SICBS conditions are consistent with those associated with increased DWFNC. This further illustrates that decreased SICBS is linked to increased DWFNC.

3.2 The role of spring snow cover over western Siberia

Then the question is how winter SICBS is connected to the DWFNC in the following spring. Figure 6 shows the regression of winter 200-hPa geopotential height and wave activity flux in the troposphere (Takaya and Nakamura 2001) on winter SICBS, in which the linear trends are removed and the SICBS is multiplied by -1 . Anomalous surface adiabatic heating induced by the reduction of sea ice in the Barents Sea tends to excite stationary Rossby waves propagating southwards from the Barents Sea through west Siberia, to north China (arrows in Fig. 6), which leads to the

anomalous anticyclonic circulation over northern Siberia and the anomalous cyclonic circulation spanning from Lake Baikal, to Mongolia, to Northeast Asia (Fig. 3). As mentioned previously, such circulation changes are associated with increased winter SAT and precipitation over Europe and western Siberia (Fig. 5a, c), leading to decreased snow cover. As shown in Fig. 6b, in decreased SICBS years, spring snow cover decreases remarkably over the western Siberia. Here we define the spring SCWS as the area-averaged snow cover in the region (54° – 60° N, 60° – 80° E). We then calculate 13-year sliding correlation coefficients between winter SICBS and spring SCWS (Fig. 6c). As we can see, winter SICBS correlates significantly with spring SCWS since the mid-1990s. That is less winter SICBS is associated with less spring SCWS.

It is well-known that snow cover affects the thermal state of the land surface and the overlying atmosphere through the snow-albedo and snow-hydrology effects (e.g., Barenett et al. 1986; Cohen and Entekhabbi 1999;

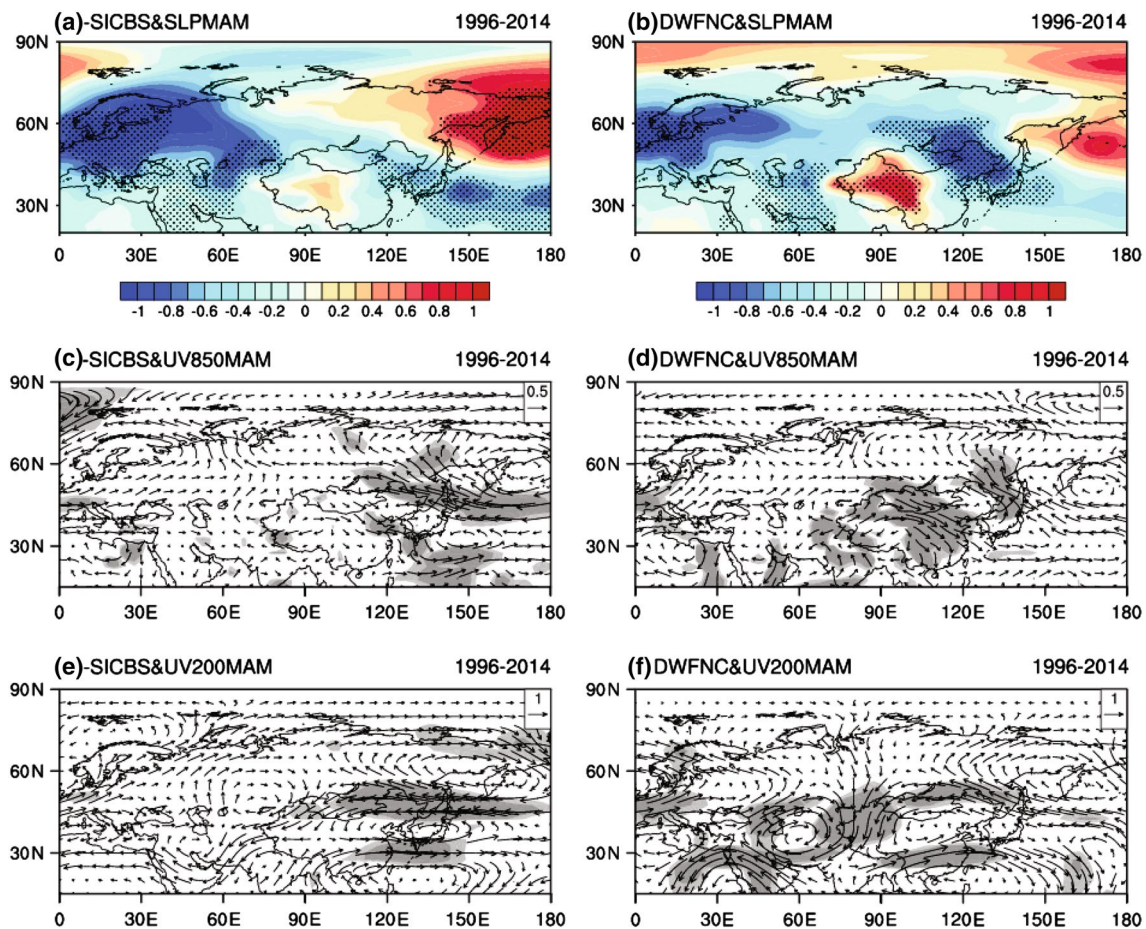


Fig. 4 As in Fig. 3, but for **a, b** gridpoint MAM-SLP, **c, d** MAM-UV 850 hPa (units: m s^{-1}), and **e, f** MAM-UV 200 hPa (units: m s^{-1})

Wu and Kirtman 2007; Zuo et al. 2012). The reduction of spring snow cover in western Siberia affects regional and remote atmospheric circulation in spring. As shown in Fig. 7, the wave activity flux associated with decreased spring SCWS propagates eastwards and southwards from western Siberia to North China. This results in a strengthened EASJ and a strong anomalous cyclonic circulation over North China, accompanied by warm SAT anomalies over western Siberia and cold SAT anomalies over North China (Fig. 7b), as well as deficient rainfall (Fig. 7c) and dry soil moisture over northern China (Fig. 7d). This is consistent with previous findings (Wu and Kirtman 2007; Zuo et al. 2012). Clearly, the features of spring atmospheric circulation and climate conditions related to spring SCWS are similar to those of winter SICBS (Figs. 6, 7). Meanwhile, the correlation between winter SICBS and spring SCWS has strengthened since the mid-1990s (Table 1). These changes indicate that SCWS plays an important role in the link between winter SICBS and spring DWFNC.

3.3 Why has winter SICBS been significantly correlated with spring DWFNC since the mid-1990s?

To answer this question, we compare the standard deviations (SDs) of interannual variability of winter SIC at each grid point in the Barents Sea for the aforementioned two periods (Fig. 8). We find that SDs of SIC in the northern Barents Sea and the Kara Sea during 1996–2014 are much larger than those during 1980–1995. We also note that the center of the SIC SDs shifts remarkably eastward to the north Barents Sea and Kara Sea during 1996–2014 relative to that during 1980–1995. This implies that the intensified and eastward shift of the center of winter SIC SDs in 1996–2014 might easily induce stronger and southward stationary Rossby wave train propagation, which influences dust-related atmospheric circulation (i.e., the East Asian upper subtropical westerly jet and low-level cyclogenesis). Consequently, these atmospheric

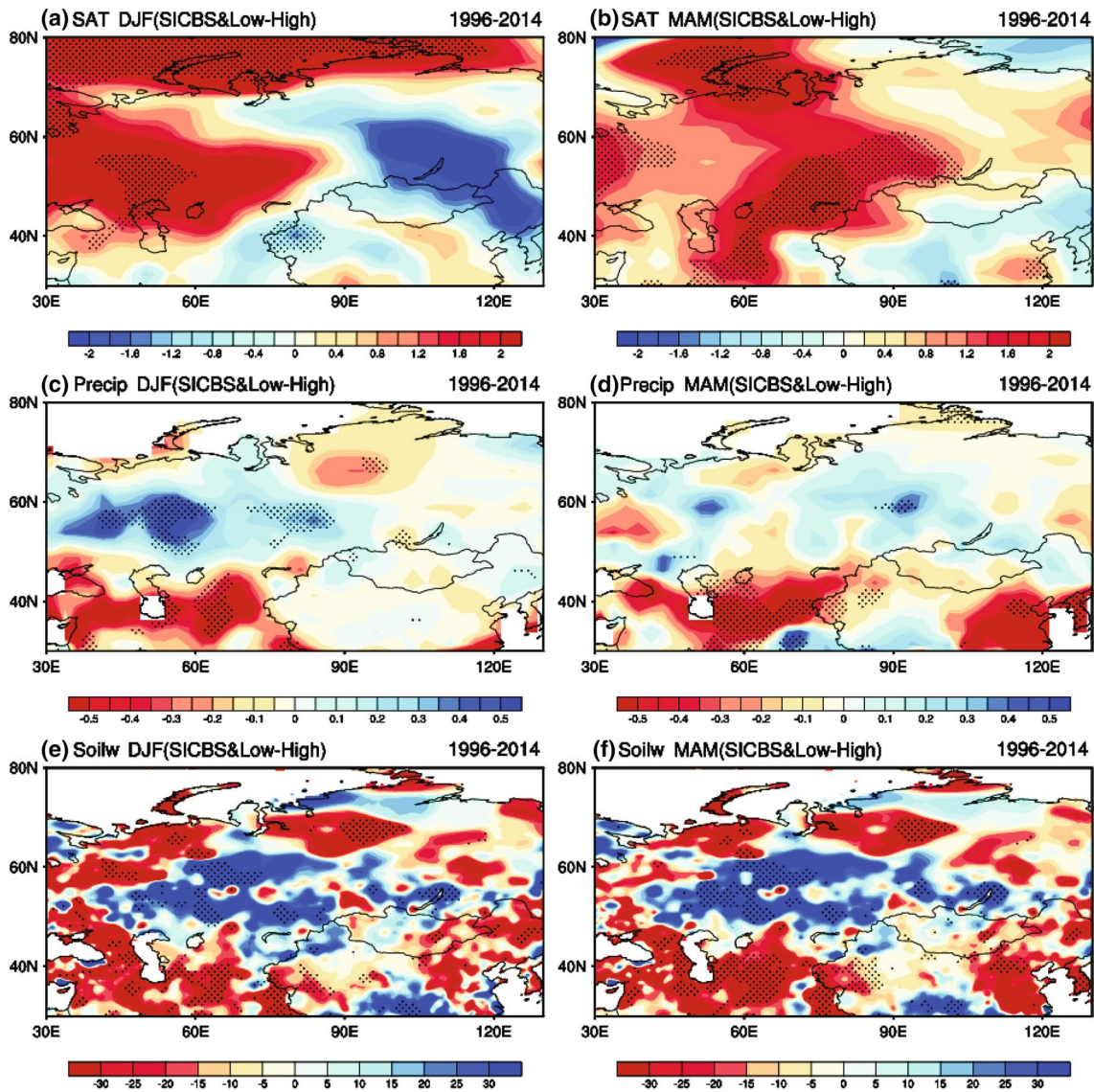


Fig. 5 Composite analysis of the climate factor differences between negative winter SICBS and positive winter SICBS (negative minus positive): **a, b** SAT (units: °C); **c, d** precipitation (units: mm/day); **e, f**

soil moisture (units: mm); **a, c, e** DJF; **b, d, f** MAM. The *dotted region* represents correlations required for significance at the 95% level, as estimated using a Student's t-test

circulation changes generate favorable climate conditions for increased DWF in 1996–2014.

Thus, we speculate that the link between winter SICBS and the spring EASJ may have intensified since the mid-1990s. Here we define the spring area-averaged zonal wind at 200 hPa over the region (25°–35°N, 100°–150°E) as the EASJ, and compute the 13-year sliding correlation between the EASJ and SICBS. Figure 8c does show that the SICBS–EASJ out-of-phase relationship becomes statistically significant (above the 95% significant level) after the mid-1990s, comparing insignificant correlation beforehand.

Following Archer and Calderia (2008), we also define the mass weighted average wind speed between 400 and

100 hPa (WS) as the intensity of the East Asian jet, which is more numerically stable and less grid-dependent than a simple maximum and minimum,

$$WS_{i,j} = \frac{\sum_{k=400\text{hPa}}^{k=100\text{hPa}} m_k * u_{i,j,k}}{\sum_{k=400\text{hPa}}^{k=100\text{hPa}} m_k}$$

where $u_{i,j,k}$ and $v_{i,j,k}$ are the daily horizontal wind components at grid-point (i, j, k), and m_k is the mass at level k. We then calculate the difference in the daily jet stream intensity over the region (25°–35°N, 100°–150°E) in MAM (91 days) between negative and positive SICBS (Fig. 8d). It appears that negative winter SICBS tends to be associated

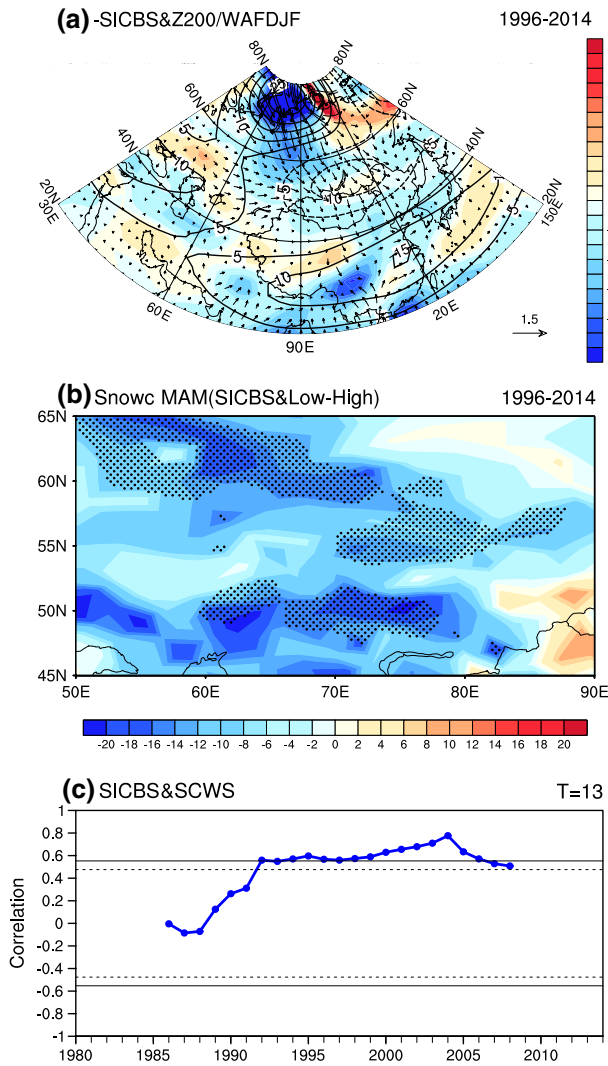


Fig. 6 **a** Linear regression of gridpoint DJF 200 hPa geopotential height (Z200) (contours; units: gpm) and wave activity flux (arrows; units: $\text{m}^2 \text{s}^{-2}$) and its divergence (shaded, units: $10^{-6} \text{m}^2 \text{s}^{-2}$) on negative winter SICBS during 1996–2014. **b** The spring snow cover anomaly over western Siberia between negative and positive winter SICBS. The dotted region (**b**) represents correlations required for significance above the 90% level, as estimated using a Student's t-test. **c** The 13-year sliding correlation coefficients between winter SICBS and spring SCWS. The dashed and solid lines denote correlations required for significance at the 90 and 95% levels, respectively, as estimated using a Student's t-test. All the linear trends have been removed in each of the plots

with a stronger EASJ in the 91 days of MAM, which further prove the relationship between negative winter SICBS and intensified spring EASJ.

The negative winter SICBS anomaly is associated with the negative NAO-like pattern in spring (Fig. 4a), accompanied by the weakened upper-level polar jet in spring, which leads to more frequent incursions of cold air from the Arctic into North China and generates strong atmospheric

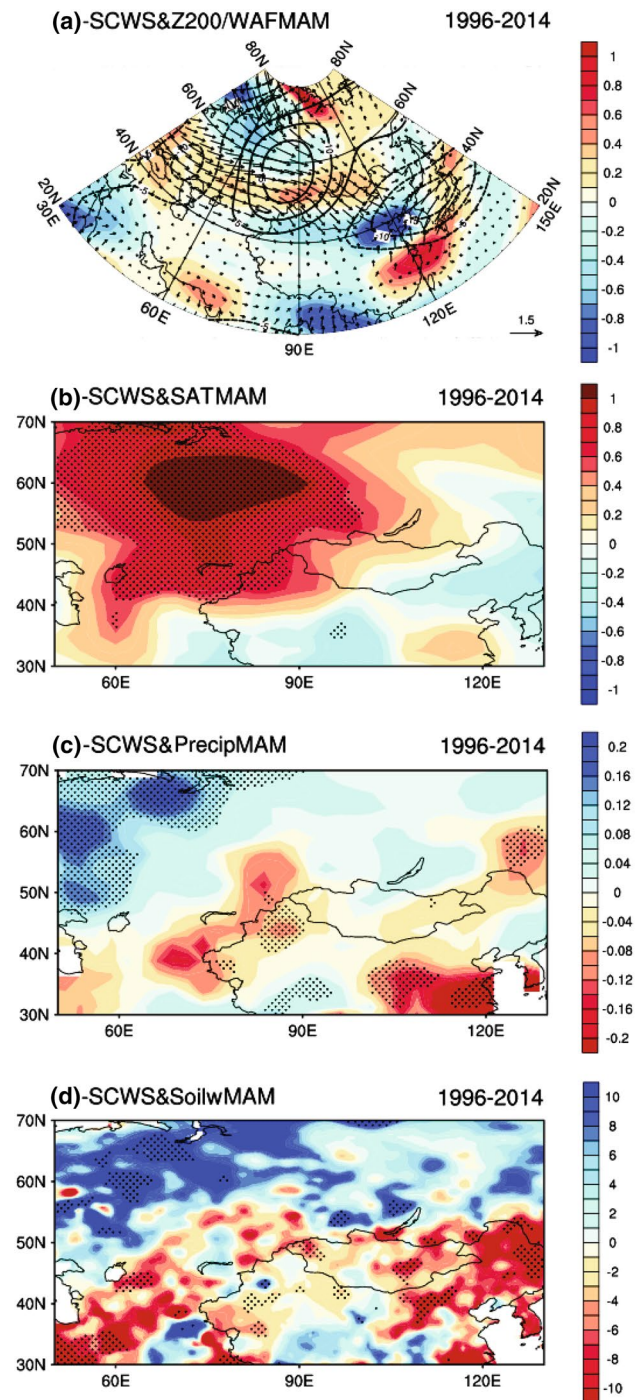


Fig. 7 **a** Linear regression of gridpoint MAM 200 hPa geopotential height (Z200) (contours; units: gpm) and wave activity flux (arrows; units: $\text{m}^2 \text{s}^{-2}$) and its divergence (shaded, units: $10^{-6} \text{m}^2 \text{s}^{-2}$). The regression of **(b)** spring SAT (units: $^{\circ}\text{C}$), **c** spring precipitation (units: mm/day), and **d** soil moisture (units: mm) on negative spring SCWS during 1996–2014. Dotted regions (**b**–**d**) represent correlations required for significance at the 95% level, as estimated using a Student's t-test. All the linear trends have been removed and SCWS multiplied by -1

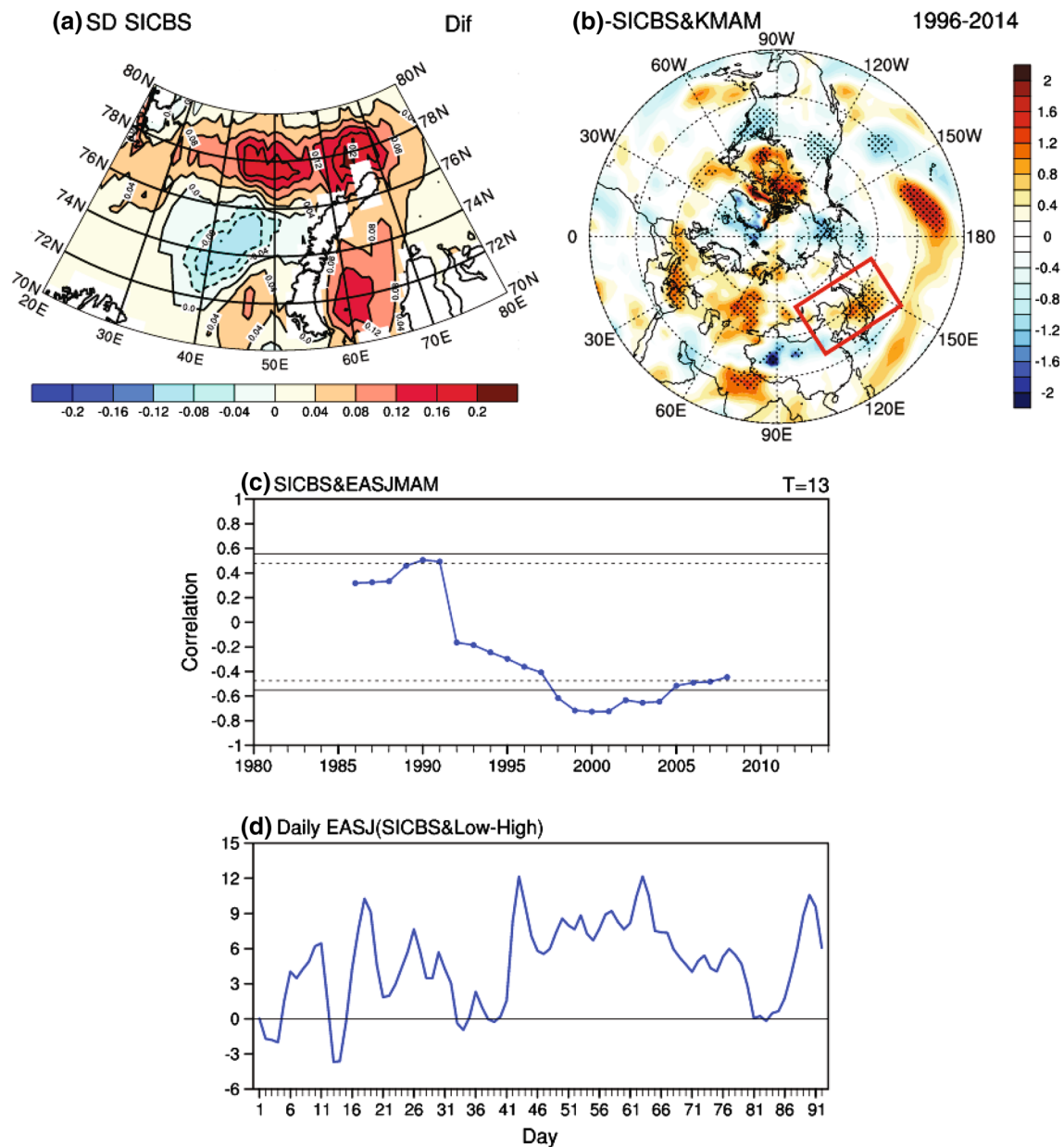


Fig. 8 **a** Interannual SDs of gridpoint SIC in the region (70°–80°N, 20°–70°E) during 1996–1995 minus those in 1980–1995. **b** Linear regression of gridpoint spring atmospheric stratification stability (calculated by the K index) on negative winter SICBS during 1996–2014. SICBS multiplied by -1. The dotted region represents correlations required for significance at 95% level, as estimated using a Student’s t-test. **c** The 13-year sliding correlation coefficients between winter SICBS and spring EASJ index. The *dashed* and *solid* lines

denote correlations required for significance at the 90 and 95% levels, respectively, as estimated using a Student’s t-test. The EASJ index is defined as area-averaged zonal wind at 200 hPa over the region (25°–35°N, 100°–150°E). **d** The difference in the daily intensity of the EASJ in MAM between negative winter SICBS and positive winter SICBS is calculated by the mass weighted average wind speed between 400 and 1000 hPa over the region (25°–35°N, 100°–50°E). All the linear trends have been removed

thermal instability in the region. To verify this, we use the K index to represent an integrated indication of atmospheric stability and moisture conditions:

$$K = (T_{850} - T_{500}) + T_{850} - (T - T_d)_{700}$$

where T_i is the i th-level air temperature and $(T_d)_j$ is the dew-point temperature at the j th level. A positive (negative) K index indicates a strong thermal instability (stability) state. As shown in Fig. 8b, negative winter SICBS anomalies are associated with positive K in spring over North China, suggesting the existence of larger atmospheric

stratification instability over that region, which leads to increase the occurrence of dust weather events.

4 Conclusion

This study finds that year-to-year variability of spring DWFNC is well correlated winter SICBS during the period 1996–2014. Our analysis shows that negative sea ice cover anomalies in the Barents Sea tend to increase cold anomalies, cyclogenesis and atmospheric thermal instability in North China. Note that the correlation between DWFNC and SICBS remains the same as the data extended to 2016 (-0.62 during 1996–2016). In light of the good relationship between DWFNC and SICBS in recent years, for the operation prediction of spring DWFNC, the winter SICBS and other dust-related climate factors should be considered together.

We reveal the possible mechanism that links winter SICBS and spring DWFNC. Firstly, SICBS anomalies exhibit good persistence from winter and spring, with high correlation between winter SICBS and spring SICBS for the period 1996–2014 (0.76 and 0.83 with and without trends, all exceeding the 99% level) (Fig. 1c). Secondly, the change in SCWS from winter to spring in response to SICBS anomalies play an important role in the link between winter SICBS and spring DWFNC, further amplifying the impacts of SICBS. Our results show that climate conditions induced by decreased winter SICBS are favorable for decreased SCWS in winter (Fig. 5) and spring (Fig. 6a, b). This is further demonstrated by the strengthened link between winter SICBS and spring SCWS since the mid-1990s (Fig. 6c). Subsequently, the reduction in spring SCWS excites the stationary Rossby wave train that propagates eastwards and southwards to north China, resulting in intensified EASJ, increased cyclogenesis and stronger westerly momentum transported downward from the upper levels in spring (Fig. 7a). The persistent reduction in SCWS in spring also results in cold anomalies, deficient spring rainfall, and dry soil in northern China (Fig. 7b–d). Such climate conditions in winter and spring encourage increased occurrence of dust weather in North China.

We then exam why winter SICBS has been significantly correlated with spring DWFNC since the mid-1990s. This is largely due to the change in the intensity of the interannual variability of SICBS. That is that the interannual standard deviation of winter SIC over large parts of the Barents Sea in 1996–2014 is found to be larger than that in 1986–1995, accompanied by eastward shift of center of actions (Fig. 8a). Consequently, the Rossby wave train associated with negative winter SICBS anomalies propagates southwards into west Siberia and northern China, more easily influencing SCWS and the dust-related atmospheric

circulation in winter and spring. These changes in atmospheric circulation further provide favorable dynamic and thermal conditions for more spring DWFNC. For instance, negative winter SICBS generates larger atmospheric stratification instability over North China necessary for increased occurrence of DWF (Fig. 8b). Therefore, the link between winter SICBS and the spring EASJ has intensified since the mid-1990s (Fig. 8c), with negative SICBS tending to enhance the EASJ. This is also demonstrated by the daily change in intensity of the EASJ in the 91 days of MAM during periods of negative SICBS anomalies (Fig. 8d).

Thus the underlying physical mechanism of the link between winter SICBS and spring DWFNC can be summarized as follows: winter SICBS reduction \rightarrow favorable winter dust climate and winter and spring SCWS reduction \rightarrow spring dust climate conditions \rightarrow DWFNC increase. Moreover, we note that both winter SICBS and DWFNC do not correlate significantly with winter and spring Niño3.4 SST index, with and without trends. Winter SICBS could therefore be applied as an independent climate predictor of spring DWFNC from the mid-1990s onwards.

Finally, why does the SIC SDs in the Barents Sea become larger in 1996–2014 than in 1980–1995? Previous studies have suggested that the gradual decline of Arctic sea ice from the 1960s to the early 1990s was driven in part by a positive trend of winter AO or NAO (Deser and Teng 2008; Comiso et al. 2008). However, the trend of AO or NAO and the rapid decline of Arctic since the mid-1990s are not consistent. We speculate that the change of SIC SDs after the mid-1990s is partly due to that the positive phase of the Atlantic multi-decadal Oscillation (AMO) has caused a rapid warming in the north Atlantic since the 1990s (Salil et al. 2011; Miles et al. 2013). The positive AMO enhances the advection of warm water from the North Atlantic to the Barents Sea. This inhibits the formation of winter SICBS, leading to less and thinner sea ice there. The atmospheric circulation change associated with the poleward propagation of Rossby waves excited by the tropical convection (Lee 2014) might be another reason. In the past three decades, the change in atmospheric circulation has led to more poleward heat and moisture transport, which contributed to surface warming and decreased sea ice cover in the Arctic by enhancing downward infrared radiation (Graversen 2006; Graversen et al. 2008; Lee 2014; Park et al. 2015). Thus the decreasing and thinning sea ice in the Barents Sea becomes more sensitive to external forcings (i.e., winds), increasing year-to-year variability. Further work is needed to improve our understanding of this issue.

As for some in phase cases but no relationship between winter SICBS and spring DWFNC during 1980–1995, they might be due to the interdecadal change of the connections between winter SICBS, spring SCWS and DWFNC identified here. This makes the variations of SICBS and DWFNC

more independently before the mid-1990s. This suggests that rather than sea ice in the Barents Sea, other physical processes play more important role in contributing to the variation of spring dust weather over North China before the mid-1990s, i.e., Arctic Oscillation, East Asian winter monsoon, vegetation coverage, ENSO.

Acknowledgements The authors are grateful to Editor and the anonymous reviewers for their insightful comments. This research was jointly supported by the National Natural Science Foundation of China (Grant Nos. 41325018, 41421004, 41575079, 41676185). The research also supported by the CAS/SAFEA International Partnership Program for creative Research Team “Regional environmental high resolution numerical simulation”.

References

- Archer CL, Calderia K (2008) Historical trends in the jet streams. *Geophys Res Lett* 30:L08803. doi:10.1029/2008GL033614
- Barnett TP, Dumenil L, Schles U, Roekler E, Latif M (1989) The effect of Eurasian snow cover on regional and global climate variation. *J Atmos Sci* 46:661–686
- Cohen J, Coauthors (2014) Recent Arctic amplification and extreme mid-latitude Weather. *Nat Geosci* 7:627–637
- Cohen J, Entekhabi D (1999) Eurasian snow cover and Northern Hemisphere climate predictability *Geophys Res Lett* 26(3):345–348
- Comiso JC, Parkinson CL, Gersten R, and Stock L (2008) Accelerated decline in the Arctic sea ice cover. *Geophys Res Lett* 35:L01703. doi:10.1029/2007GL031972
- Deser C, Teng H (2008) Evolution of Arctic sea ice concentration trends and the role of atmospheric circulation forcing during 1979–2007. *Geophys Res Lett* 35:L02504. doi:10.1029/2007GL032023
- Fan K and Wang HJ (2004) Antarctic Oscillation and the dust weather frequency in North China. *Geophysics Res Lett* 31:L10201. doi:10.1029/2004GL019465.
- Fan K, Wang HJ (2006) The interannual variability of dust weather frequency in Beijing and its global atmospheric circulation. *Chin J Geophys* 49:890–897
- Fan K and Wang HJ (2007a) Dust storms in North China in 2002: a case study of the low frequency oscillation. *Adv Atmos Sci* 24(1):15–23
- Fan K, Wang HJ (2007b) Simulation on the AAO anomaly and its influence on the Northern Hemispheric circulation in boreal winter and spring. *Chin J Geophys* 50(2):397–403
- Fan K, Xie ZM, Xu ZQ (2016) Two different periods of high dust weather frequency in northern China, 016 Vol. 9 (4):263–269. doi:10.1080/16742834.2016.1176300
- Francis J, Vavrus S (2012) Evidence linking Arctic amplification to extreme weather in mid-latitudes. *Geophys Res Lett* 39:L06801
- Gao YQ, Sun JQ, Li F, et al. (2015) Arctic Sea ice and Eurasian Climate: a review. *Adv Atmos Sci* 32:92–114
- Gong DY, Mao R, Shi PJ et al (2007) Correlation between east Asian dust storm frequency and PNA. *Geophys Res Lett* 34:L14710. doi:10.1029/2007GL029944
- Graversen (2006) Do changes in the midlatitude circulation have any impact on the Arctic surface air temperature trend?. *J Clim* 19:5422–5438
- Graversen G, Mauritsen T, Tjernström M et al (2008) Vertical structure of recent Arctic warming. *Nature* 451:53–56
- Inoue J, Hori M (2012) The role of Barents Sea ice in the wintertime cyclone Track and emergence of a warm-Arctic and cold-Siberian Anomaly. *J Clim* 25:2561–2568
- Kalnay E, Coauthors (1996) The NCEP/NCAR 40-year reanalysis project. *Bull Am Meteorol Soc* 77:437–471
- Kang DJ, Wang HJ (2005) Analysis on the decadal scale variation of the dust storm in North China. *Science in China (series D)* (in Chinese) 35 (11):1096–1102
- Kurosaki Y, Mikami M (2003) Recent frequent dust events and their relation to surface wind in East Asia. *Geophys Res Lett* 30:1736. doi:10.1029/2003GL017261
- Lang XM (2008) Prediction model for spring dust weather frequency in North China. *Sci China (series D)* 51:709–720
- Lee S (2014) A theory for polar amplification from a general circulation perspective. *Asia-Pac J Atmos Sci* 50:31–43
- Liu JP, Curry JA, Wang HJ et al (2012) Impact of declining Arctic sea ice on winter snowfall. *Proc Natl Acad Sci USA* 109:4074–4079
- Miles MW, Divine DV, Furevik T, Jansen E, Moros M, Ogilvie AEJ (2013) A signal of persistent Atlantic multidecadal variability in Arctic sea ice. *Geophys Res Lett*. doi:10.1002/2013GL058084
- Park D, Lee S, Feldstein M (2015) Attribution of the recent winter sea ice decline over the Atlantic sector of the Arctic Ocean*. *J Clim* 28:4027–4033
- Petoukhov and Semenov V (2010) A link between reduced Berents-Kara sea ice and cold winter extremes over northern continents. *J Geophys Res* 115:D21111. doi:10.1029/2009Jd013568
- Qian WH, Quan LS, Shao SY (2002) Variations of the dust storm in China and its climatic control. *J Clim* 15:1216–1229
- Robinson DA, Dewey KF, Heim R (1993) Global snow cover monitoring: an update. *Bull Am Meteorol Soc* 74:1689–1696
- Salil M, Zhang R, Delworth TL (2011) Impact of the Atlantic Meridional overturning circulation (AMOC) on Arctic surface air temperature and sea ice variability. *J Clim* 24:6573–6581
- Stroeve JM, Holland M, Meier W, et al. (2007) Arctic sea ice decline: faster than forecast. *Geophys Res Lett* 34:L109501. doi:10.1029/2007GL029703
- Takaya K, Nakamura H (2001) A formulation of a phase-independent wave-activity flux for stationary and migratory quasigeostrophic eddies on a zonally varying basic flow. *J Atmos Sci* 58(6):608–627
- Uccellini LW (1986) The possible influence of upstream upper-Level Baroclinic Processes on the development of the AEII storm. *Mon Weather Rev* 114:1019–1026
- Wang HJ, HP Chen, Liu JP (2015) Arctic Sea ice decline intensified haze pollution in eastern China. *Atmos Ocean Sci Lett* 8:1–9
- Wu RG, Kirtman BP (2007) Observed relationship of spring and summer East Asian rainfall with winter and Spring Eurasian snow. *J Climate* 20:1285–1304
- Wu BY, Huang RH, Gao DY (1999) The impacts of the variation of the se-ice extend in the Kara Sea and Barents Sea in the winter on the winter Monsoon over east Asia (in Chinese). *Chines. J Atmos Sci* 23:268–275
- Wu YF, Zhang RJ, Han ZW, et al. (2010) Relationship between East Asian monsoon and dust weather frequency over Beijing. *Adv Atmos Sci* 27:1389–1398
- Yang S, Lau KM, Kim KM (2002) Variations of the East Asian jet stream and Asian-Pacific- American winter climate winter climate anomalies. *J Clim* 15:306–325
- Zhang RJ, Han ZW, Wang MX et al. (2002) Dust storm weather in China: new characteristics and origins (in Chinese). *Quat Sci* 22:374–380
- Zhao CS Dabu X, Li Y (2004) Relationship between Climatic factors and dust storm frequency in Inner Mongolia of China. *Geophys Res Lett* 31:L01103. doi:10.1029/2003GI018351

- Zhu CW, Wang B, Qian WH (2008) Why do dust storms decrease in northern China concurrently with the recent global warming? *Geophys Res Lett* 35:L18702. doi:[10.1029/2008GL034886](https://doi.org/10.1029/2008GL034886)
- Zou XK, Zhai PM (2004) Relationship between vegetation coverage and spring dust storms over northern China. *J Geophys Res Atmos* 109(D3). doi:[10.1029/2003JD003913](https://doi.org/10.1029/2003JD003913)
- Zuo ZY, Zhang RH, Wu BY, Rong XY (2012) Decadal variability in springtime snow over Eurasia: relation with circulation and possible influence on spring time rainfall over China. *Int J Climatol* 32:1336–1345